Iranian Journal of Medical Physics

ijmp.mums.ac.ir

IJMP

Investigation of Noise Level and Spatial Resolution of CT Images Filtered with a Selective Mean Filter and Its Comparison to an Adaptive Statistical Iterative Reconstruction

Ummu Mar'atu Zahro[1], Choirul Anam[1,*], Wahyu Setia Budi[1], Pandji Triadyaksa[1], Jhon Hadearon Saragih[1], Dito Andi Rukmana[2]

1. Department of Physics, Faculty of Sciences and Mathematics, Diponegoro University, Jl. Prof. Soedarto SH, Tembalang, Semarang 50275, Central Java, Indonesia
2. Department of Radiology, Indriati Hospital Solo Baru, Jl. Palem Raya, Dusun III, Sukoharjo 57552, Central Java, Indonesia

ARTICLE INFO

Article type:
Original Paper

Article history:
Received: May 16, 2020
Accepted: Jun 26, 2020

Keywords:
Computed Tomography
Image Quality
Algorithms
Image Processing
Selective Mean Filter
Adaptive Statistical Iterative Reconstruction

ABSTRACT

Introduction: A simple noise reduction algorithm, i.e. a selective mean filter (SMF), had been previously introduced. The aim of this study is to investigate the image qualities filtered by a SMF and its comparison to an adaptive statistical iterative reconstruction (ASIR).

Material and Methods: To assess the basic image quality, an American Association of Physicists in Medicine Computed Tomography (AAPM CT) performance phantom was used. The phantom was scanned by 128 Multiple Slices Computed Tomography. The tube current varied from 50 mA to 100, 150, and 200 mA. The images of a phantom were reconstructed by filtered back projection (FBP) followed by SMF and ASIR (20, 40, 60, 80, and 100%). The image quality assessment was in terms of noise level, noise power spectrum (NPS), and modulation transfer function (MTF).

Results: The noise level and NPS of SMF was similar with ASIR 100%. The values of the MTF_{10} of the ASIR filter at any level and SMF were comparable. The MTF_{10} values of ASIR 60%, and SMF with 50 mA (low) were 0.76 ± 0.02 and 0.75 ± 0.02 cycle/mm, respectively. Meanwhile, the MTF_{10} of ASIR 60% and SMF with 200 mA (high) were 0.74 ± 0.00 and 0.73 ± 0.00 cycles/mm, respectively.

Conclusion: Our results indicated that the performance of the SMF in reducing noise is equivalent to the maximum level of ASIR strength, i.e., ASIR 100%.

► *Please cite this article as:*
Zahro UM, Anam CH, Budi WS, Triadyaksa P, Saragih JH, Rukmana DA. Investigation of Noise Level and Spatial Resolution of CT Images Filtered with a Selective Mean Filter and Its Comparison to an Adaptive Statistical Iterative Reconstruction. Iran J Med Phys 2021; 18: 374-383. 10.22038/IJMP.2020.48813.1786.

Introduction

Computed tomography (CT) scanner provides images that contain patient's detailed and precise anatomical information for accurate clinical diagnosis. However, the use of CT scanner also causes a high radiation dose on patients that can increase the incidence of cancer. A method to reduce the radiation dose without deteriorating the diagnostic image quality is known as dose optimization. Many studies have been carried out to optimize CT dose, such as, implementing a tube current modulation, shielding, proper patient positioning, and gantry tilting [1-4]. However, the effect of these interventions can vary on different patients and examination conditions [5]. Another effective method to optimize CT dose is implementing noise reduction filters in both sinogram and image spaces [4]. The process is described as follows: setting a relatively low CT exposure parameter (mA) to make patient receive a lower radiation dose, with a consequence of increasing the image noise, followed by reducing the noise by applying a noise reduction filter. It is known that methods in noise reduction always cause a decrease in image's spatial resolution, which can cause a misinterpretation in diagnosing diseases and abnormalities [6]. Therefore, several methods have been proposed to maintain the spatial resolution quality when reducing noise [7–16].

Many algorithms for noise reduction have been proposed, including mean filter (MF) [9], adaptive mean filter (AMF) [8,9], and bilateral filter (BF) [10–13]. A study reported the ability of MF and AMF in significantly reducing image noise, although the spatial resolution of the image significantly decreased [14]. Meanwhile, the BF, known as a non-iterative adaptive smoothing filter, maintains object's edges while reducing noise [13] and reportedly can increase the peak signal to noise ratio (PSNR) for about 32% with still maintaining its image spatial resolution [10]. But the use of BF requires a relatively heavy computation due to its complex mathematics

**Corresponding Author:* Tel: +62-24-74680822; Email: anam@fisika.fsm.undip.ac.id

construction. On average, it takes about 25 s to process a 512 x 512 CT image [10].

CT manufacturers also provide noise reduction algorithms known as iterative reconstruction (IR) with different names such as *adaptive statistical iterative reconstruction* (ASIR) from GE, *sinogram-affirmed iterative reconstruction* (SAFIRE) from Siemens, *iDose* from Philips, and *adaptive iterative dose reduction 3D* (AIDR3D) from Toshiba [15]. On its application, IR is able to reduce the noise while maintaining the spatial resolution of the image [3,16], that makes it potential to produce a good image quality with lower dose. However, IR technique is not always installed in the CT scanner and needs extra cost to acquire it [16]. Therefore, a simple noise reduction algorithm with capabilities similar to IR can be a solution to many institutions, which do not have IR software yet. A study by Anam *et al.* introduced a simple, fast, and easily implemented algorithm of noise reduction, known as a selective mean filter (SMF) [17]. The SMF produced similar results of image's spatial resolution compared to the original image [17]. These results suggest the performance of SMF in maintaining the spatial resolution with reducing noise. Therefore, this study aimed to investigate several quantitative image quality parameters from using SMF and compare them to IR of one CT manufacturer (ASIR).

Materials and Methods

Phantom, CT and software

An American Association of Physicists in Medicine Computed Tomography (AAPM CT) Performance phantom (Model 610, CIRS, Virginia, US) was scanned using a 128 Slice Computed Tomography (Revolution Evo, GE Healthcare, Waukesha, WI) with its scanning parameters tabulated in Table 1. The image quality in terms of noise level, noise power spectrum (NPS), and spatial resolution (modulation transfer function, MTF) were measured. The images were reconstructed by the filtered back projection (FBP) technique and ASIR. We used five different levels of the ASIR strength, i.e., 20, 40, 60, 80, and 100%. The images of FBP were then filtered using the SMF technique. Meanwhile, in the SMF technique, images were denoised in another computer using Matlab software (Mathworks Inc., Natick, Massachusetts, USA). In this study, we used Acer Nitro 5 Intel Core i5-8300H 2.3 GHz with 8GB RAM, Graphic Processor Unit (GPU) Nvidia Geforce GTX 1050 4GB under the Windows 10 Home operating system with SSD M.2 NVMe 2280 256GB.

Table 1. The Acquisition Parameters for Image Acquisition

Acquisition mode	Axial
Tube potential (kVp)	120
Tube current (mA)	50, 100, 150, 200
Pitch	0.984
Rotation time (s)	2
Detector coverage (mm)	2.5
Slice thickness (mm)	5

SMF Method

The SMF algorithm is one of the noise reduction methods based on the mean filter (MF) technique. However, not all pixels in a particular kernel area are included in the average calculation, but they are selectively chosen based on a threshold value (h). The threshold value was determined based on image noise (σ). In this study, the h was set as 3σ. The selection of pixel with position of (i, j) in a kernel with central position of (x, y) was determined by the following equation [17]:

$$I'(x+i,y+j) = \begin{cases} I(x+i,y+j), & if \quad |I(x,y)-I(x+i,y+j)| \le h \\ 0, & if \quad |I(x,y)-I(x+i,y+j)| > h \end{cases} \tag{1}$$

After that, the mean value in every pixel of (x, y) was calculated by equation (2) [17].

$$I_s(x,y) = \frac{\sum_{i=-\frac{n-1}{2},j=-\frac{m-1}{2}}^{+\frac{n-1}{2},+\frac{m-1}{2}} I'(x+i,y+j)}{N'(x,y)} \tag{2}$$

Where $N'(x,y)$ is the number of selected pixels within kernel area.

ASIR

The standard method for image reconstruction is FBP. CT manufactures have introduced an algorithm based on IR to reduce radiation doses while maintaining image quality. One of the IR methods is ASIR, which is an additional software on the CT scanner with additional costs. ASIR is an IR technique based on a repetitive reconstruction of a set of image data that leads to a better representation of the object being imaged [18]. ASIR works on raw data space modelling of the fluctuation in the projection measurement and the noise characteristics of the scanned object. Its performance is fast and can be achieved by using a high-end fast computer technology; thus, it is suitable for clinical applications.

ASIR uses an image from the FBP algorithm as initial image to be iteratively reconstructed. By this initial image, ASIR uses an algebraic matrix to change the measured value of each pixel (y) into a new estimate of the pixel value (y'). This pixel value is directly computed to get an ideal value of noise in the image. This process is successively repeated until the ideal value of the pixel is finally found. The ASIR process is divided into three main steps. First, a forward-projection of the object estimate to produce artificial raw data. Second, comparison between the artificial raw data and the measured raw data for correction. Third, a back-projection of the correction data onto the image of the object estimate. The iteration loop stops when the correction to the estimated image is small enough, or the image quality criteria met, or a certain number of iterations is reached [19, 20]. There are various levels of denoising strength of the ASIR, i.e., 10, 20, 30, 40, 50, 60, 70, 80, 90, and 100%.

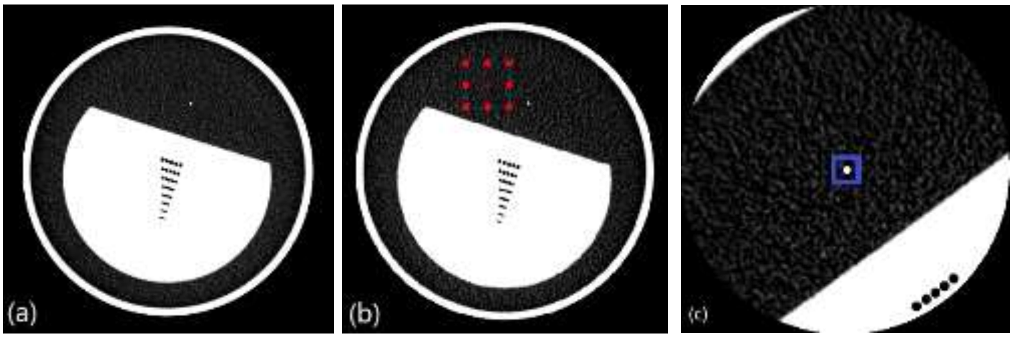

Figure 1. (a) Image of the resolution insert of AAPM CT performance phantom for measuring spatial resolution. (b) Position of ROI for NPS calculation, and (c) Image of the phantom with 10 cm field of view (FOV). The FOV was decreased for MTF measurement to investigate the high spatial resolution capability of the CT system.

Image Quality Assessment

The image qualities of FBP, ASIR, and SMF in terms of noise level, noise power spectrum (NPS), and modulation transfer function (MTF) were assessed.

Noise was measured using an automated noise calculation algorithm by MATLAB software (R2019b, MathWorks Inc., Natick, US). An automatic noise calculation was performed by using the sliding window of about 1 cm^2 to create the standard deviation map (SDM). The noise was identified as the smallest SD from the SDM because the smallest SD is the most homogeneous area within the image [21].

NPS is a useful metric to describe the spatial frequency content of noise and plays an important role in analyzing the performance of the imaging system [22,23]. The NPS is calculated by equation (3) [24]:

$$NPS\ (u,v) = \frac{d_x d_y}{N_x N_y} |\mathcal{F}[I(x,y) - P(x,y)]|^2 \quad (3)$$

where u represents spatial frequency in the x-directions, v represents spatial frequency in the y-directions, d_x and d_y are pixel size (mm), N_x and N_y represent the number of pixels in the x and y direction of the ROI, $\mathcal{F}$ denotes the 2D Fourier transform, $I(x,y)$ is the pixel value (HU) of a ROI at position (x,y), and $P(x,y)$ is a 2nd order polynomial fit of $I(x,y)$. In this study, the NPS curves were generated using ImQuest software. A rectangular region of interest (ROI) of about 31 × 31 mm was placed in homogeneous area on phantom images to calculate NPS (Figure 1(b)).

MTF values were measured using an automated algorithm in MATLAB. MTF is basically an objective way to assess the visibility of any object on an image. It is a spatial resolution evaluation matrix imaging system that is often used in CT imaging. The MTF curve provides information across all spatial frequencies of a CT image [25]. MTF can be measured with a disk image of a cylindrical phantom (such as the American College of Radiology (ACR) phantom) by taking into account the line spread function (LSF), point spread function (PSF), or edge spread function (ESF) [26, 27]. Recently, Anam *et al.* [27] reported a simple software to automatically calculate MTF to be used as part of a quality assurance program for CT. The MTF curve was obtained from the Fourier transform of the LSF curve. The MTF curve was determined by the following equation [27]:

$$MTF(f) = |F(LSF(x))| = \left| \int_{-\infty}^{+\infty} [LSF(x) e^{-2\pi jxf}]\, dx \right| \quad (4)$$

where f denotes the spatial frequency and F indicates the Fourier transform.

The resolution insert of the AAPM CT performance phantom is shown in Figure 1 (a) and is reconstructed with a 25,5 cm FOV. However, to investigate the high spatial resolution capability of the CT system, the FOV was decreased to 10 cm (Figure 1(c)). A rectangular ROI of 32 × 32 pixels was placed in the center of the wire image (Figure 1(c)). MTF was measured at three slices of images. To get the quantitative value of spatial resolution, MTF_{10} and MTF_{50} were computed from all images.

Results

The noises of FBP images and filtered images (ASIR and SMF) for various tube currents are shown in Figure 2. As depicted, the noise levels increase when tube current decreases as expected. The noise levels decrease with the increase of ASIR level in every tube current value. The noise levels of SMF were almost similar to ASIR 100% noise levels in every tube current.

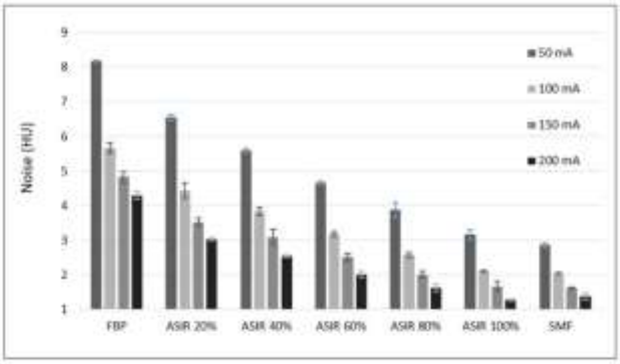

Figure 2. The graphs of noises in the AAPM phantom images with different tube currents for FBP images and filtered images by ASIR with various levels and standard SMF

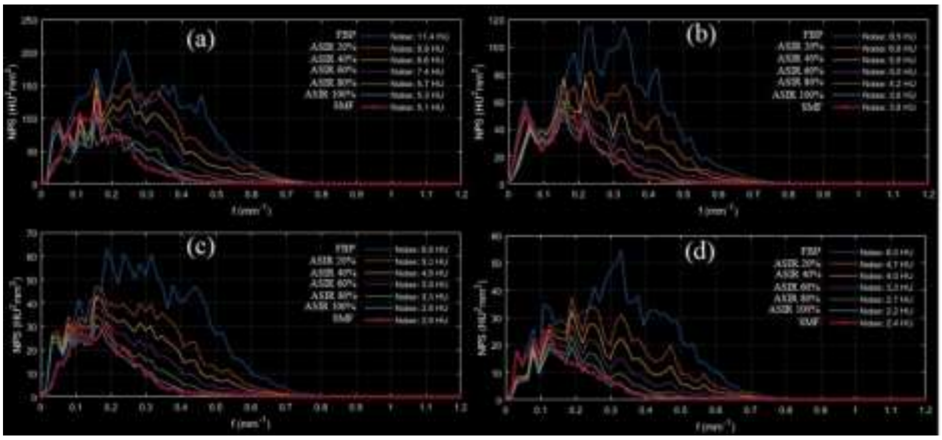

Figure 3. NPS curves of FBP images and filtered images using ASIR and SMF for various tube currents (mA): (a) 50 mA, (b) 100 mA, (c) 150 mA, and (d) 200 mA

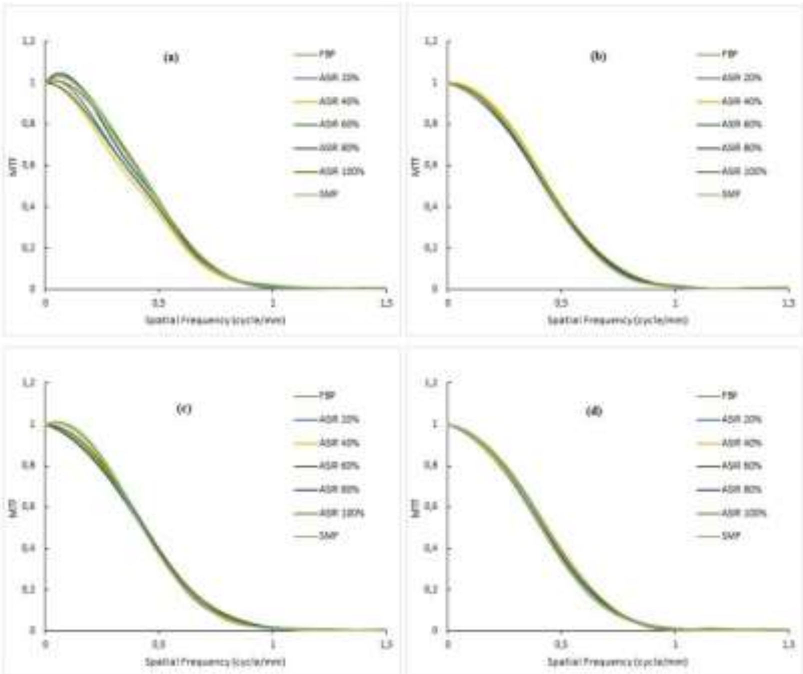

Figure 4. The MTF curves of FBP images and filtered images using ASIR and SMF for various tube currents: (a) 50 mA, (b) 100 mA, (c) 150 mA, and (d) 200 mA

The NPS curves of FBP, ASIR (20, 40, 60, 80, and 100%), and SMF for various tube currents are shown in Figure 3. As can be seen, an increase in the tube current causes a decrease in the noise level. Also, the noise levels of ASIR and SMF significantly decreased compared to FBP. The SMF produced the lowest NPS compared to any level of ASIR. All four images for various tube currents had the same pattern.

The MTF curves for original images (FBP) and the images filtered with ASIR (20, 40, 60, 80, and 100%) and SMF for various tube currents of 50, 100, 150, and 200 mA are shown in Figure 4. As shown, all images have comparable MTF indicated by an overlap in the MTFs curves. Figure 4 shows that maximum MTF curves go beyond a unity, which is because of the effect of reconstruction filter on the point spread function (PSF). If the normalized PSF completely follows the Gaussian distribution (i.e., there is no negative value in the normalized PSF), then the maximum MTF value is 1. However, due to the effect of reconstruction filter, there are negative values in both tiles of the normalized PSF curve, which causes the peak of the MTF curve to be more than 1.

Figure 4 also shows that in small tube currents, fluctuations in the MTF curves are indeed relatively large due to its high noise. This phenomenon has been reported in a previous study [28]. Therefore, accurate MTF measurements require relatively large tube currents (above 100 mA).

From these MTF curves, the MTF_{10} and MTF_{50} values could be derived. The values of MTF_{10} and MTF_{50} for original images (FBP) and the images filtered with ASIR (20, 40, 60, 80, and 100%) and SMF for various tube currents of 50, 100, 150, and 200 mA are tabulated in Table 2. Again, the data show that the values of MTF_{10} and MTF_{50} for all images are comparable. These results indicate that the SMF preserves the spatial resolution of the images, while it reduces the noises of images, as expected.

Table 2. MTF_{10} and MTF_{50} values for AAPM images for various mA and filter algorithms

Tube current (mA)	Algorithms	MTF_{10} (Cycle/mm)	MTF_{50} (Cycle/mm)
	FBP	0.747 ± 0.03	0.408 ± 0.05
	ASIR 20%	0.736 ± 0.01	0.417 ± 0.03
	ASIR 40%	0.740 ± 0.01	0.420 ± 0.01
50	ASIR 60%	0.755 ± 0.02	0.428 ± 0.03
	ASIR 80%	0.759 ± 0.01	0.437 ± 0.02
	ASIR 100%	0.774 ± 0.02	0.451 ± 0.05
	SMF	0.748 ± 0.02	0.446 ± 0.04
	FBP	0.739 ± 0.00	0.433 ± 0.01
	ASIR 20%	0.747 ± 0.00	0.434 ± 0.02
	ASIR 40%	0.755 ± 0.01	0.435 ± 0.04
100	ASIR 60%	0.761 ± 0.01	0.444 ± 0.01
	ASIR 80%	0.767 ± 0.01	0.440 ± 0.03
	ASIR 100%	0.769 ± 0.00	0.448 ± 0.01
	SMF	0.739 ± 0.00	0.434 ± 0.01
	FBP	0.738 ± 0.01	0.424 ± 0.01
	ASIR 20%	0.745 ± 0.02	0.427 ± 0.02
	ASIR 40%	0.750 ± 0.02	0.430 ± 0.02
150	ASIR 60%	0.755 ± 0.02	0.432 ± 0.02
	ASIR 80%	0.760 ± 0.01	0.435 ± 0.01
	ASIR 100%	0.770 ± 0.01	0.441 ± 0.01
	SMF	0.743 ± 0.01	0.431 ± 0.00
	FBP	0.730 ± 0.00	0.416 ± 0.00
	ASIR 20%	0.735 ± 0.00	0.417 ± 0.01
	ASIR 40%	0.740 ± 0.01	0.427 ± 0.01
200	ASIR 60%	0.741 ± 0.00	0.428 ± 0.01
	ASIR 80%	0.745 ± 0.00	0.430 ± 0.00
	ASIR 100%	0.749 ± 0.00	0.435 ± 0.01
	SMF	0.732 ± 0.00	0.416 ± 0.00

Discussion

As mentioned in the introduction, many dose optimization techniques have been used to reduce the dose of CT. Implementation of noise reduction filters is one of the effective techniques for dose optimization [4–8]. Anam *et al.* [17] reported that SMF has the potential to reduce patient doses by up to 75% without reducing the spatial resolution of the original image. It was also reported that the SMF algorithm is 54% superior to the

BF in terms of computational speed with comparable image spatial resolution results.

In the current study, we investigated the image qualities of SMF and compared them to IR method, i.e., the ASIR. Our findings confirmed previous studies reporting that ASIR can significantly reduce the noise level of imaging, and therefore it might reduce the dose [28–32]. It was reported that ASIR reduces the dose up to 60% without decreasing its image quality [33]. Chen *et al.* [34] reported that ASIR 50% reduced noise by approximately 35% compared with FBP. In this study, we found that, on average, SMF reduced noise by more than 65% compared with FBP in each tube current (mA). It was found that the noise level of SMF was lower than the noise levels of the ASIR 20-80%. The noise level of SMF seems to be similar with the noise level of ASIR 100%. Similarly, it was found that the NPS curve of the SMF is equivalent to the ASIR 100%. This indicated that the performance of SMF in reducing noise is equivalent to the maximum level of ASIR performance. The pattern of noise reduction looked alike in every mA group.

As Figure 2 shows, the noise level of SMF was similar with ASIR 100%. Numerically, at 200 mA, the noise level of SMF was 10% lower than ASIR 100%. However, at 50 mA, the noise level of ASIR 100% was 7% lower than SMF. For 100 mA and 150 mA, it had the same difference percentage of noise level, i.e., the noise of SMF was 3% lower than ASIR 100%.

We compared the SMF noise level, which is close to the ASIR noise level on other tube currents. Noise level of the 50 mA SMF is close to 200 mA ASIR 20%. Noise level of the 100 mA SMF is equivalent to 200 mA ASIR 60%, 150 mA ASIR 80%, and 100 mA ASIR 100%. Noise level of the 150 mA SMF is equivalent to 200 mA ASIR 80% and 150 mA ASIR 100%. Noise level of the 200 mA SMF was close enough to 200 mA ASIR 100%. Based on data, it is clear that SMF filter is comparable to certain ASIR levels at certain tube currents.

Several studies have been carried out to investigate the impact of spatial resolution as a function of ASIR [25, 35, 36]. In the current study, we analyzed the image spatial resolution for FBP, ASIR, and SMF. The average difference percentage of MTF_{10} between SMF and FBP was 0.2% in every mA. Based on the noise level value, we compared the difference percentage of MTF_{10} between SMF and ASIR 100% in every mA, and the average difference percentage was 3.3%. Therefore, the MTF_{10} and MTF_{50} values of SMF, ASIR, and FBP are very similar. In agreement with our findings, Anam *et al.* [17] reported that MTFs of the filtered images using SMF are very similar to the FBP. Another study by Richard *et al.* [25] reported that there is no dependence between MTF with linearity setting. However, Hussain *et al.* [18] reported that ASIR strength more than 50% resulted in vague images, and Yanagawa *et al.* [35] showed that there are partial obscurity and subtle opacities at ASIR 100% image.

Our findings confirm that results of the SMF are comparable to those from the ASIR. The advantage is that SMF can be an alternative for institutions with CT scanner not equipped with IR software, such as ASIR. The main limitation of the IR technique is its long reconstruction time that needs a sophisticated high speed computation technology. Silva *et al.* [36] reported that ASIR reconstruction needs longer time compared to FBP reconstruction for a standard abdominopelvic CT. While Anam *et al.* [17] found that using netbook (Lenovo Ideapad 330S with intel Core i5), the computing time of the SMF was 1.635 ± 0.045 seconds for one slice of image. In this study, we did not carry out a qualitative assessment involving radiologists in clinical images. Further studies are required to compare the image quality (quantitative and qualitative assessments) between SMF and IR from other CT manufactures.

Conclusion

The use of the SMF method significantly reduced the image noise while maintaining the spatial resolution of the image. It is found that the noise and spatial resolution of images filtered by the SMF are comparable to those from ASIR. Therefore, the SMF filters can be used in the low-dose CT and they could be an alternative for institutions with CT scanner not equipped with IR software, such as ASIR.

Acknowledgment

This work was funded by the Riset Publikasi International Bereputasi Tinggi (RPIBT), Diponegoro University (Contract Numbers: 329-116/UN7.6.1/ PP/2021)

References

1. Ibrahim M, Parmar H, Christodoulou E, Mukherji S. Raise the bar and lower the dose: current and future strategies for radiation dose reduction in head and neck imaging. American Journal of Neuroradiology. 2014 Apr 1;35(4):619-24.
2. Irdawati Y, Sutanto H, Anam C, Fujibuchi T, Zahroh F, Dougherty G. Development of a novel artifact-free eye shield based on silicon rubber-lead composition in the CT examination of the head. Journal of Radiological Protection. 2019 Sep 24;39(4):991.
3. Anam C, Fujibuchi T, Toyoda T, Sato N, Haryanto F, Widita R, et al. The impact of head miscentering on the eye lens dose in CT scanning: Phantoms study. InJournal of Physics: Conference Series. 2019 Apr 1; 1204:012022.
4. Yabuuchi H, Kamitani T, Sagiyama K, Yamasaki Y, Matsuura Y, Hino T, et al. Clinical application of radiation dose reduction for head and neck CT. European journal of radiology. 2018 Oct 1;107:209-15.
5. Perisinakis K, Raissaki M, Tzedakis A, Theocharopoulos N, Damilakis J, Gourtsoyiannis N. Reduction of eye lens radiation dose by orbital bismuth shielding in pediatric patients undergoing CT of the head: a Monte Carlo study. Medical physics. 2005 Apr;32(4):1024-30.
6. Anam C, Fujibuchi T, Budi WS, Haryanto F, Dougherty G. An algorithm for automated

modulation transfer function measurement using an edge of a PMMA phantom: Impact of field of view on spatial resolution of CT images. Journal of applied clinical medical physics. 2018 Nov;19(6):244-52.

7. Kalra MK, Maher MM, Sahani DV, Blake MA, Hahn PF, Avinash GB, Toth, et al. Low-dose CT of the abdomen: evaluation of image improvement with use of noise reduction filters‒pilot study. Radiology. 2003 Jul;228(1):251-6.
8. Hilts M, Jirasek A. Adaptive mean filtering for noise reduction in CT polymer gel dosimetry. Medical physics. 2008 Jan;35(1):344-55.
9. Anam C, Haryanto F, Widita R, Arif I. New noise reduction method for reducing CT scan dose: Combining Wiener filtering and edge detection algorithm. In AIP Conference Proceedings. 2015 Sep 30; 1677: 040004.
10. Al-Hinnawi AR, Daear M, Huwaijah S. Assessment of bilateral filter on 1/2-dose chest-pelvis CT views. Radiological physics and technology. 2013 Jul;6(2):385-98.
11. Dong G, Acton ST. On the convergence of bilateral filter for edge-preserving image smoothing. IEEE Signal Processing Letters. 2007 Aug 13;14(9):617-20.
12. Zhang M, Gunturk BK. Multiresolution bilateral filtering for image denoising. IEEE Transactions on image processing. 2008 Nov 11;17(12):2324-33.
13. Tomasi C, Manduchi R. Bilateral filtering for gray and color images. In Sixth international conference on computer vision.1998 Jan 7; 39-846.
14. Lee IH, Kang DU, Shin SW, Lee RG, Park JK, Lee Y. Development of a total variation noise reduction algorithm for chest digital tomosynthesis. Optik. 2019 Jan 1;176:384-93.
15. Andersen HK, Völgyes D, Martinsen AC. Image quality with iterative reconstruction techniques in CT of the lungs‒A phantom study. European journal of radiology open. 2018 Jan 1;5:35-40.
16. Suyudi I, Anam C, Sutanto H, Triadyaksa P, Fujibuchi T. Comparisons of hounsfield unit linearity between images reconstructed using an adaptive iterative dose reduction (AIDR) and a filter back-projection (FBP) techniques. Journal of Biomedical Physics & Engineering. 2020 Apr;10(2):215-24.
17. Anam C, Adi K, Sutanto H, Arifin Z, Budi WS, Fujibuchi T, Dougherty G. Noise reduction in CT images using a selective mean filter. Journal of Biomedical Physics & Engineering. 2020 Oct;10(5):623-34..
18. Hussain FA, Mail N, Shamy AM, Alghamdi S, Saoudi A. A qualitative and quantitative analysis of radiation dose and image quality of computed tomography images using adaptive statistical iterative reconstruction. Journal of applied clinical medical physics. 2016 May;17(3):419-32.
19. Seeram E. Computed Tomography-E-Book: Physical Principles, Clinical Applications, and Quality Control. Elsevier Health Sciences. 2015 Sep 2.
20. Barca P, Giannelli M, Fantacci ME, Caramella D. Evaluation of the Imaging Properties of a CT Scanner with the Adaptive Statistical Iterative Reconstruction Algorithm-Noise, Contrast and Spatial Resolution Properties of CT Images Reconstructed at Different Blending Levels. InInternational Conference on Biomedical Electronics and Devices. 2017;2: 200-6.
21. Anam C, Budi WS, Adi K, Sutanto H, Haryanto F, Ali MH, et al. Assessment of patient dose and noise level of clinical CT images: automated measurements. Journal of Radiological Protection. 2019 Jul 5;39(3):783.
22. Dolly S, Chen HC, Anastasio M, Mutic S, Li H. Practical considerations for noise power spectra estimation for clinical CT scanners. Journal of applied clinical medical physics. 2016 May;17(3):392-407.
23. Williams MB, Mangiafico PA, Simoni PU. Noise power spectra of images from digital mammography detectors. Medical physics. 1999 Jul;26(7):1279-93.
24. Samei E, Bakalyar D, Boedeker KL, Brady S, Fan J, Leng S, et al. Performance evaluation of computed tomography systems: summary of AAPM task group 233. Medical physics. 2019 Nov;46(11):e735-56.
25. Richard S, Husarik DB, Yadava G, Murphy SN, Samei E. Towards task-based assessment of CT performance: system and object MTF across different reconstruction algorithms. Medical physics. 2012 Jul;39(7Part1):4115-22.
26. Takenaga T, Katsuragawa S, Goto M, Hatemura M, Uchiyama Y, Shiraishi J. Modulation transfer function measurement of CT images by use of a circular edge method with a logistic curve-fitting technique. Radiological physics and technology. 2015 Jan 1;8(1):53-9.
27. Anam C, Fujibuchi T, Haryanto F, Budi WS, Sutanto H, Adi K, et al. Automated MTF measurement in CT images with a simple wire phantom. Polish Journal of Medical Physics and Engineering. 2019;25(3):179-87.
28. Greess H, Lutze J, Nömayr A, Wolf H, Hothorn T, Kalender WA, el al. Dose reduction in subsecond multislice spiral CT examination of children by online tube current modulation. European radiology. 2004 Jun;14(6):995-9.
29. Paterson A, Frush DP. Dose reduction in paediatric MDCT: general principles. Clinical radiology. 2007 Jun 1;62(6):507-17.
30. Parakh A, Macri F, Sahani D. Dual-energy computed tomography: dose reduction, series reduction, and contrast load reduction in dual-energy computed tomography. Radiologic Clinics. 2018 Jul 1;56(4):601-24.
31. Brady SL, Yee BS, Kaufman RA. Characterization of adaptive statistical iterative reconstruction algorithm for dose reduction in CT: a pediatric oncology perspective. Medical physics. 2012 Sep;39(9):5520-31.
32. Dodge CT, Tamm EP, Cody DD, Liu X, Jensen CT, Wei W, at al. Performance evaluation of iterative reconstruction algorithms for achieving CT radiation dose reduction‒a phantom study. Journal of applied clinical medical physics. 2016 Mar;17(2):511-31.
33. Willemink MJ, Leiner T, de Jong PA, de Heer LM, Nievelstein RA, Schilham AM, et al. Iterative reconstruction techniques for computed tomography part 2: initial results in dose reduction and image quality. European radiology. 2013 Jun;23(6):1632-42.
34. Chen B, Marin D, Richard S, Husarik D, Nelson R, Samei E. Precision of iodine quantification in

hepatic CT: effects of iterative reconstruction with various imaging parameters. American Journal of Roentgenology. 2013 May;200(5):W475-82.

35. Yanagawa M, Honda O, Yoshida S, Kikuyama A, Inoue A, Sumikawa H, et al. Adaptive statistical iterative reconstruction technique for pulmonary CT: image quality of the cadaveric lung on standard-and reduced-dose CT. Academic radiology. 2010 Oct 1;17(10):1259-66.
36. Silva AC, Lawder HJ, Hara A, Kujak J, Pavlicek W. Innovations in CT dose reduction strategy: application of the adaptive statistical iterative reconstruction algorithm. American Journal of Roentgenology. 2010 Jan;194(1):191-9.